Computed strength of uni-axially loaded battened columns composed of four cold formed angles

M.A. El Aghoury[1], A.H. Salem[2], M.T. Hanna[3], E.A. Amoush[4]

Abstract

Cold-formed steel structural members play a great role in modern steel structures due to their high strength and light weight. The behavior and strength of battened column members composed of slender angle sections are mainly governed by local buckling of angle legs or torsional buckling of the whole angle between batten plates. Moreover, local buckling depends on the interaction between the width-thickness ratio of angle leg, overall slenderness ratios of angle between batten plates as well as the overall slenderness ratios of the columns. A nonlinear finite element model was developed to study the effect of the aforementioned factors on the ultimate capacity of uni-axially loaded columns. A parametric study was performed on a group of battened beam-columns with variable angle legs width-thickness ratios, angle local slenderness ratios, and column overall slenderness ratios. In addition detailed measurements for the geometric and material imperfections that arise from manufacturing and handling is presented together with there effects on the ultimate strength. Finally, interactive axial load-bending moment curves were produced and compared with that of different design rules.

1. Introduction
Current trends in steel construction are to use high yield steels and thin cross-sections to achieve light weight structures. However, the combination of high yield stress and high plate slenderness leads to local instability with reduced section capacities in compression and bending. Moreover, the pattern of the geometric and material imperfections might be different in thin cold-formed sections from that in compact hot rolled sections. Due to the slenderness of plates that form the section, local geometric defects with relative values may arise in those plates. Furthermore, the shape and values of residual stress pattern change because of the different thermal treatments.

In this paper measurements of the member's initial geometric imperfections as well as the internal residual stresses are described for battened members composed of four equal cold-formed slender angles. In addition, a numerical nonlinear finite element model is developed to

---

[1] Professor of Steel Structures, Ain Shams University, Egypt <aghoury_tc@yahoo.com>
[2] Professor of Steel Structures, Ain Shams University, Egypt <aghoury_tc@yahoo.com>
[3] Associate Professor, Housing and Building National Research Center, Egypt <m_tawfick2003@yahoo.com>
[4] Assistant Professor, Higher Technological Institute, Egypt<essamamoush2008@yahoo.com>

study the effect of the mentioned factors on the ultimate capacities of such members when subjected to axial compressive force with different eccentricities. Finally, axial load-bending moment interaction diagrams are constructed, and the predicted strengths are compared with Eurocode-3 (2001) and AISI (2007) design codes.

Trahair (2007) studied the behavior of a single angle loaded eccentrically in a plane inclined to the principal planes. The strengths of such beams are affected by local buckling effects on their section resistances, as well as lateral buckling effects and torsion on the interaction between the major and minor axes moments during biaxial loading. He concluded that despite the apparent simplicity of single angle beams, their behaviour is often complex and their strengths are difficult to predict. He provided a design method which is rational, consistent and economical. Hasham and Rasmussen (2002) studied the strength of thin-walled I-sections under combined compression and major axis bending. They found that, the shape of interaction curves for slender beam-columns failing by local and in-plane bending was slightly convex, also the shape of the interaction curves for non-compact and compact cross-sections failing by in-plane bending was also convex. El Aghoury et al. (2010) carried out an experimental program to test a group of battened columns with different cross-sections, which had different outstanding leg width-thickness ratios, slenderness ratios of angle between batten plates and overall slenderness of columns. The deformed shapes observed consist of series of local buckling waves with half wave length nearly equal to the spacing between batten plates. After these buckling waves had happened, the specimens continue carrying additional loads until they fail. For short columns, local buckling (global torsion of single angle) was the observed failure mode, however, for medium columns the interactive local buckling and overall flexural buckling governed the failure modes. Also, Murray and Ghada Elmahdy (1993), carried out an experimental and theoretical study to investigate the behaviour of battened columns constructed of standard steel channel sections. A combination of equivalent slenderness ratios and limitations to the slenderness ratios of the main members between batten plates (interconnectors) were provided. Also many other researchers dealt with the problem of imperfections either describing there patterns or studying there effects on the ultimate strength. Sridharan and Ali (1988) illustrated the role of imperfections in producing scatter in the prediction of the ultimate capacity of the thin walled columns. Weng and Pekoz (1990), presented a detailed description of the experimental study of residual stresses in cold formed steel sections. Results showed that the residual stresses in cold-formed sections were quite different from those in hot-rolled shapes. It was also shown that this type of stresses may weaken not only the overall column buckling strength but also the local buckling strength of the component plate elements of the section. Schafer and Pekoz, (1998), characterized the geometric imperfections and residual stress patterns of channel and Z cold-formed sections aiming to determine practical distributions and magnitudes for use in numerical modeling of such sections.

2. Parametric Study Variables.
A series of battened columns composed of equally spaced four cold-formed angles (square open box) is studied, see Fig.1. These columns have different outer dimension B, different outstanding leg width-thickness ratios, $\lambda_b=b/t$, different slenderness of a single angle between batten plates $\lambda_z=L_z/i_z$ and different overall slenderness ratios, $\lambda_c=L/i$. The angle leg width-thickness ratios λ_b are taken 20 and 40 to cover the limits given by EC3 and AISI-2007. The ratio of the single angle slenderness between batten plates, λ_z, with respect to the column overall slenderness ratio,

λ_c; for each cross-section is taken equal to $0.667\lambda_c$ and λ_c. Finally, members with different lengths were chosen to have wide range of overall column slenderness ratios, λ_c, which ranged from 15 to 250.

3. Finite Element Model

The finite element model included thin-shell elements with four nodes and six degrees of freedom per node to model the battened columns as shown in Fig 1. Both large deflection analysis and bilinear elasto-plastic material model have been incorporated in a non-linear finite element model, where ANSYS finite element package (1989), was used. The elastic modulus of elasticity and yield stress of the steel material were considered as 210,000 MPa and 240 MPa; respectively. The shear modulus was taken equal to 81,000 MPa. A bilinear stress-strain curve obeying von Mises yield criterion was adopted for material modeling. The load was incrementally increased through successive load steps. Newton-Raphson iterations were used in solving the nonlinear system of equations.
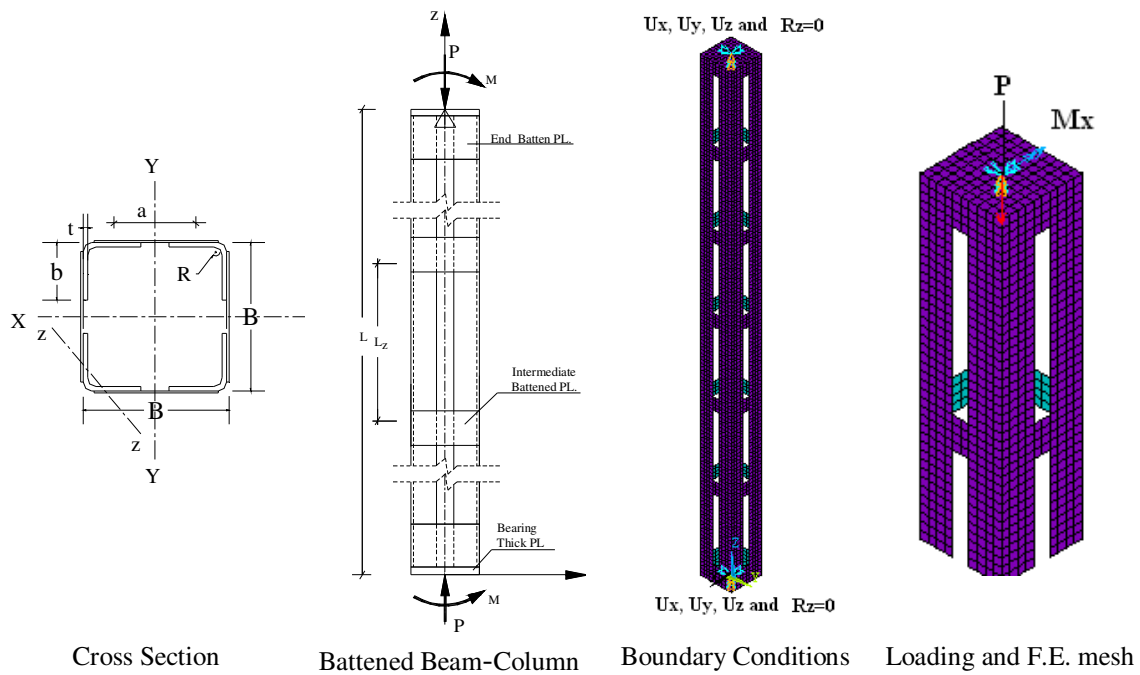

Figure 1: Finite Element Model and Boundary Condition

The end conditions for beam-column elastic line were treated as pinned. However, warping of the end column cross section is restrained due to the provision of thick end plate along with a square frame comprised of four angles. The nodes in the center of the square end plates are prevented from both rotations about Z and Y-axes and translations in both X, Y and Z directions. In this study, there are three cases of loading considered in the analyzed models. These cases are listed as follows: in the first case, the member is subjected to axial compressive force at the centroid of the battened column section to get the maximum axial capacity of the member P_{uo}. In the second case, the member is subjected to bending moment at its ends to cause a single curvature about major axis to get maximum bending capacity of the member M_{uo}. In the third

case, the member is subjected to axial compression P_u and equal end moments about the major axis causing single curvature in the members (uni-axially loaded beam-column).

3.1 Measurements of initial imperfections

Imperfections are classified into geometric and material imperfections (residual stresses). A fundamental knowledge about the imperfections that exist in cold-formed steel members is essential information for accurate determination of the ultimate capacities of these members. In the following section the local as well as global geometric imperfections of twenty specimens, in addition to the residual stresses in two cold formed angles are measured.

The notation of geometrical imperfections includes all the shape variations in structural members with reference to their ideal geometry. They may be transverse when related to the cross section, local imperfections, or longitudinal whenever they concern the bar axis overall imperfections. The geometric imperfections were measured by a digital vernier with an accuracy of .01mm. The specimens were placed on a horizontal table as depicted in Fig.2. Readings were taken from 7 locations spaced by S= L'/6 along the specimen length, where L' is the length of the specimen between the end batten plates. At each location, readings were taken at two points on each leg. The first point is the tip point, while the second one is the corner. Due to roundness of the corner, measurements were taken at distance away from the corner (5to10mm). Each reading was taken several times to ensure the verticality of the vernier.
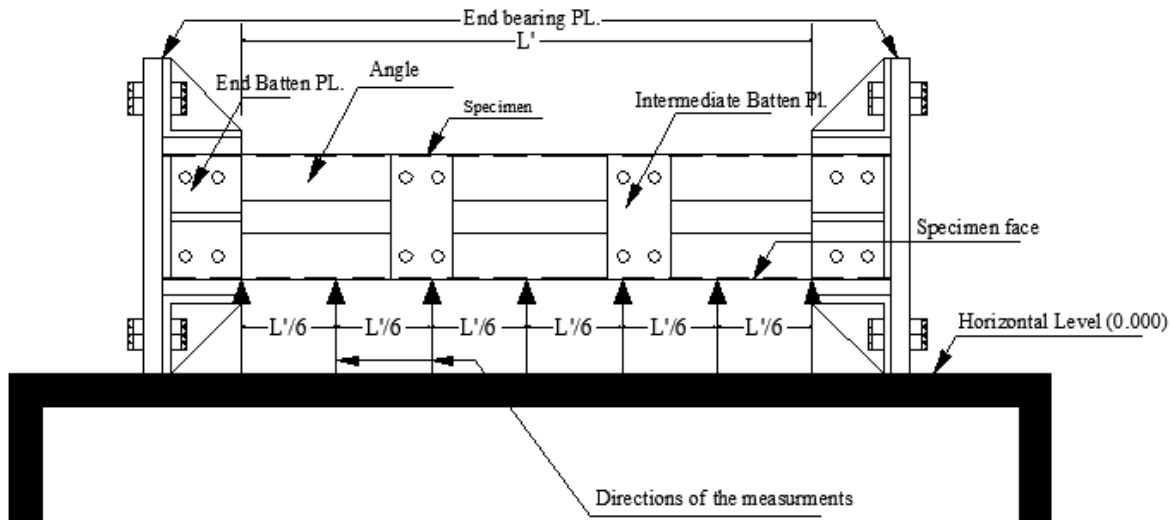

Figure 2: Technique of measuring geometric imperfections.

Overall imperfections are the average of subtracting the readings taken at the corner points from those at the end sections. However, local imperfections were calculated by subtracting the readings at the tip points from the corner points at each location of reading. The overall imperfection shape of specimen having λ_b=20, λ_z=0.667λ_c, λ_c=30 , are given in Fig. 3, while Fig. 4 shows the out of squareness shape which is indicated as dotted lines at three different locations (L'/3, L'/2, 2L'/3).
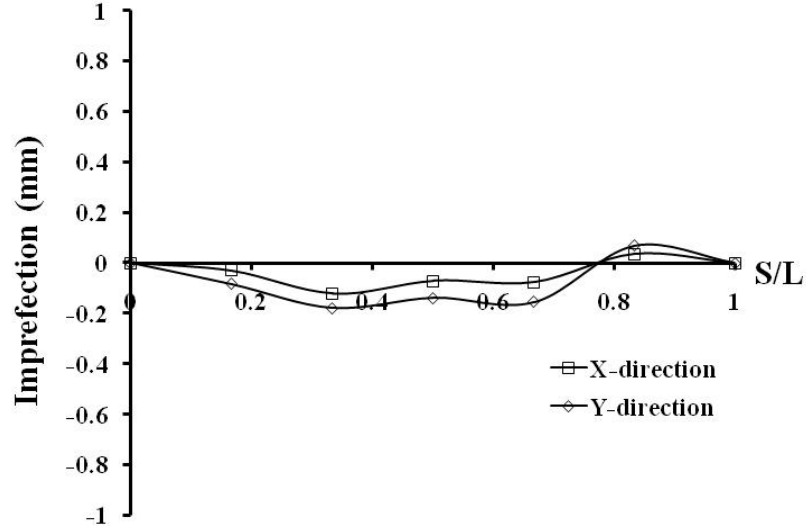
Figure 3: Average overall imperfection profile in X & Y directions, specimen (λ_b=20, λ_z=0.667λ_c, λ_c=30)
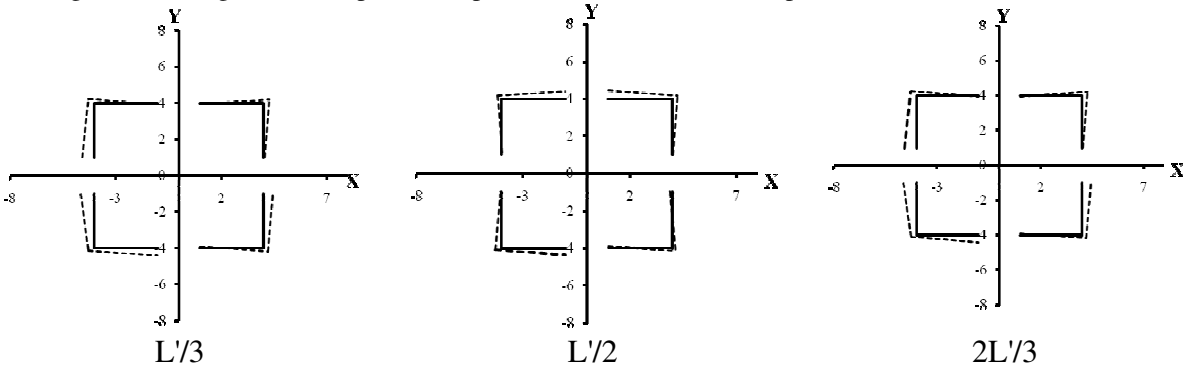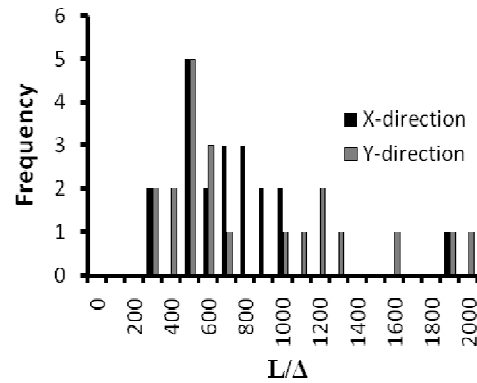

| L'/3 | L'/2 | 2L'/3 |

Figure 4: Out of squareness shape of specimen (λ_b=20, λ_z=0.667λ_c, λ_c=30) at three different locations.

Fig. 5 shows the frequencies of the local imperfection, b/ δ, and overall imperfection, L/ Δ. It is seen that the average local imperfections range from b/50 to b/20 with highest frequency value of b/15. In addition, the overall geometric imperfections range from L/1600 to L/284 and also the highest frequency value is L/500.
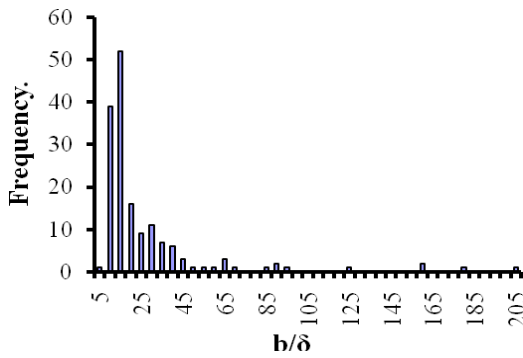
a) Local imperfection values   b) Overall imperfection values

Figure 5: Frequencies of the measured local and overall imperfection values

Two angles with length equal to 200 mm are prepared to measure the internal residual stresses. Dimensions of the angles are 30x30x1.5mm, and 40x40x1.5mm. The residual stresses are determined using the method of sectioning, Ballio and Mazzolani (1983), in which the specimens are marked into strips as shown in Fig. 6. The angle specimen was divided into 10 mm width strips. The middle 100 mm part from the 200 mm specimen length was used for the actual measurements. The strips were marked on both sides of the angle specimen. The residual strain was measured by using a digital micrometer with an accuracy of .01mm.

a) Angles are divided into strips   b) Two marks on each side of the strip 100mm distant apart.   c) Photo shows the strip numbers
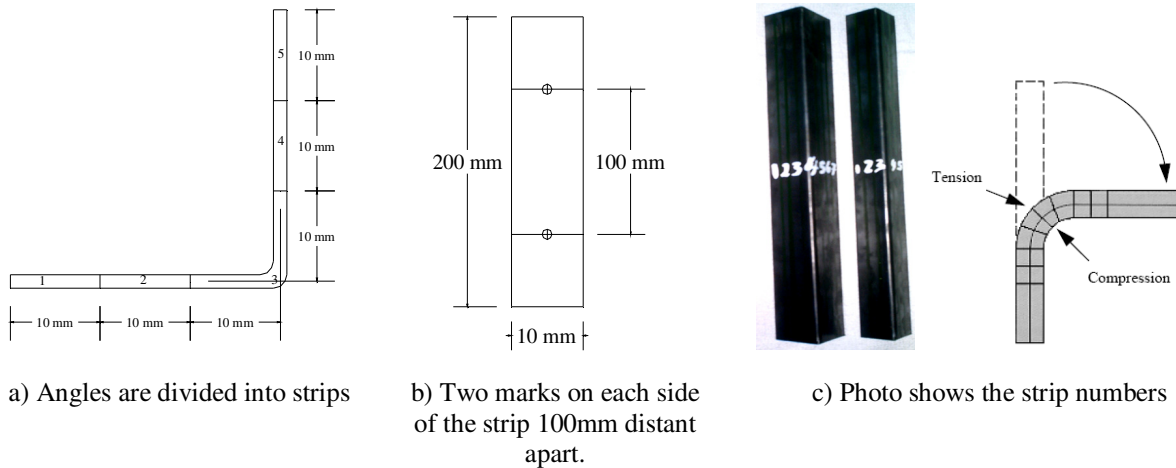
Figure 6: Technique of measuring residual stresses.

Initial readings on both sides of all strips had been recorded. Then the strips were cut slowly using a band saw with a coolant flowing continuously. After cutting the strips, another set of readings were recorded on both sides of each individual strip.

30x30x1.5   40x40x1.5   30x30x1.5   40x40x1.5

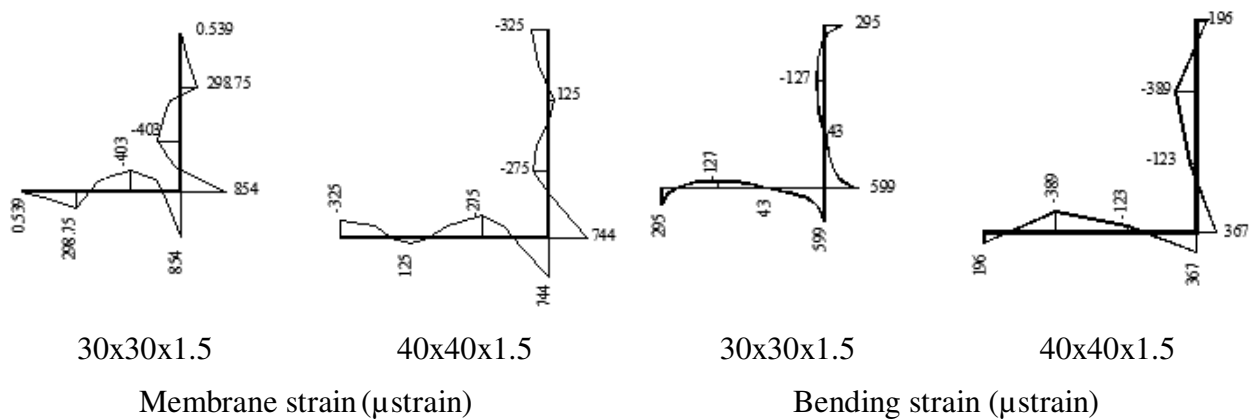Membrane strain (μstrain)   Bending strain (μstrain)

Figure 7: Membrane and bending residual strains.

The residual strain is defined as the difference between the initial gage length before cutting and final gage length after cutting divided by the final gage length after cutting. The residual stress is determined as the product of the measured residual strains and the elastic modulus using the stress-strain curves. The membrane and bending residual strains measured for the selected cross sections are drawn in Fig. 7. Membrane strains are calculated, similar to Popovic, et. al.(1999), as the average of readings taken from the two sides of the strips, while the bending strains are the

difference between the readings taken from the two sides divided by two. It is evident that membrane tensile residual strains are concentrated near the corner and at the tip of the angle legs. However, the average highest values are at the corner ranges from 750 to 850 microstrain. In addition, membrane compressive residual strains are spread near the middle of the angle legs with average value ranging from 275 to 400 microstrain. This pattern is nearly similar to that measured by Popovic, et. al.(1999).

4. Discussion of the Results

4.1 Effect of Initial Imperfections

Salem et al. (2004) found that the ultimate strength is sensitive to overall geometric imperfections rather than the local geometric imperfections. Therefore, overall geometric imperfections are considered only by modeling the member with one half-sine wave along its whole length. The maximum amplitude at the member mid-length, Δ, is the overall imperfection value as shown in Fig.8. In addition, an average residual strain and stress patterns are assumed based on the measured patterns as depicted in Fig.9. The patterns are characterized by tensile stress near the tip and corner points with average values of $0.186F_y$ and $0.7F_y$, respectively, and a compressive stress in the remained part with average value of $0.22F_y$. The average membrane residual stress pattern is applied in the finite element model as pre-stress, which is kept constant while the external applied force increases up to the failure load.
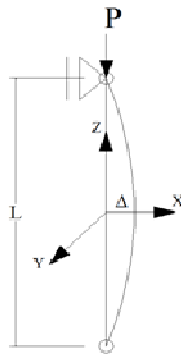

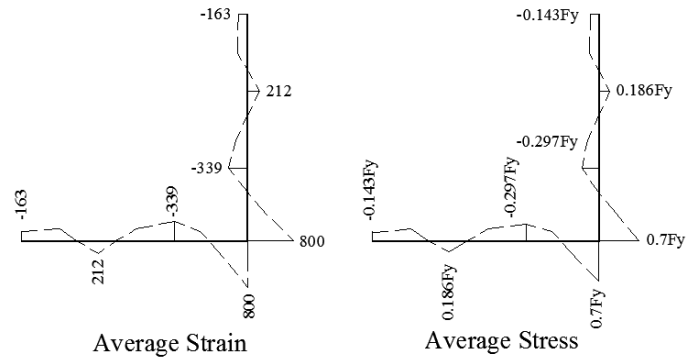Figure 8: Assumed geometric imperfections model.

Figure 9: Assumed average membrane residual strain and stresses patterns.

The effect of the initial overall geometric imperfections on the ultimate strength of specimen having $\lambda_b=20$, $\lambda_z=0.667\lambda_c$, $\lambda_c=30$ for several types of loading (axial, uni-axial, and bi-axial) is shown in Fig. 10, where the ratio P_u/P_y is plotted as function of the imperfection value, Δ. Note that P_u is the ultimate load and P_y is the yield load (P_y = gross area of 4 angles multiplied by yielding stress, F_y). Also note, in uni-axial loading, the axial load is applied with eccentricity, $e_x/B=1/8$, while it is applied with eccentricities of $e_x/B=e_y/B=1/8$ for bi-axial loading, where "B" is the total width of the specimen. For all cases, the curvature of the overall imperfection shape is similar to that due to the applied eccentricities. The figure reflects that, generally, the ultimate strength decreases by increasing the overall imperfection value. In axial loadings, the ratios P_u/P_y decrease from 0.74 to 0.62 (16%), when the overall imperfection values increase from L/1500 to L/500. However, in uni-axial and bi-axial loading the reduction in strength is nearly the same since the ratio P_u/P_y decreases from .538 to .472 (12%), and from .341 to .301 (12%) for uni-

axial and bi-axial loading, respectively, for the same increase in the overall imperfection values. Eventually, it can be concluded that the effect of the overall geometric imperfections becomes less important when the columns are subjected to eccentric loads.
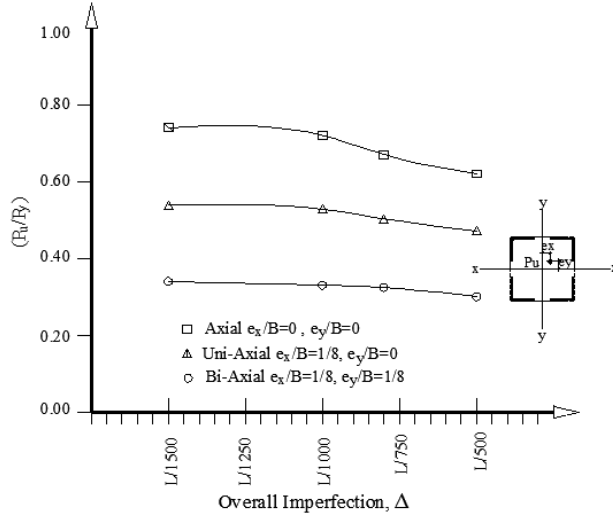

Figure 10: Relationship between (P_u/P_y) and different initial overall geometric imperfections for specimen with λ_b=20, λ_z=0.667λ_c, λ_c=30.
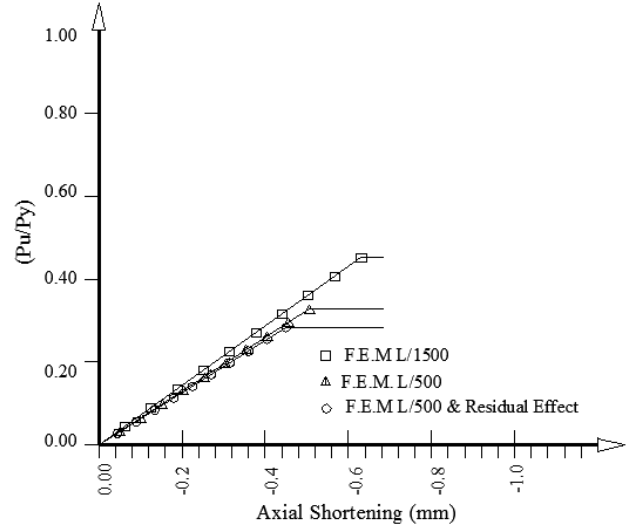
Figure 11: Relationship between (P_u/P_y) and axial shortening for specimen with λ_b=26, λ_z=0.667λ_c, λ_c=58.

To assess the effect of residual stresses, the specimen having λ_b=26, λ_z=0.667λ_c, λ_c=58 had been modeled considering the average residual stress pattern that is mentioned in the previous section. The relation between the ratio P_u/P_y and the axial shorting of the axially loaded specimen is drawn in Fig. 11 for different cases of geometric imperfections and residual stresses. It is conspicuous that the ratio (P_u/P_y) decreases from .45 to .34 (24 %) when the overall imperfection increases from L/1500 to L/500. Moreover, the ratio decreases further to be .298 when the residual stress pattern is considered in-addition to overall imperfection value of L/500. Consequently, it can be concluded that the residual stresses reduce the ultimate strength by about 15%.

4.2 Stresses Distributions at Failure Loads
For uni-axially loaded beam-columns the stress distribution across the sections with width-thickness ratio of the angle legs λ_b=20 and 40, along with slenderness ratio of the single angle between battens λ_z=0.667λ_c are drawn for different overall slenderness ratios of columns in Fig.12. The figure reflects that for short columns (λ_c=15), Local buckling waves did not happened for the case having λ_b=20 while these waves are appeared in one angle leg when λ_b=40. Since the stress distribution becomes nonlinear across on leg for the other leg the stresses are almost linear. However, local buckling is clearly observed in both legs of angles on the compression side of the deformed column which has λ_b=40 and λ_c=100 & 200.
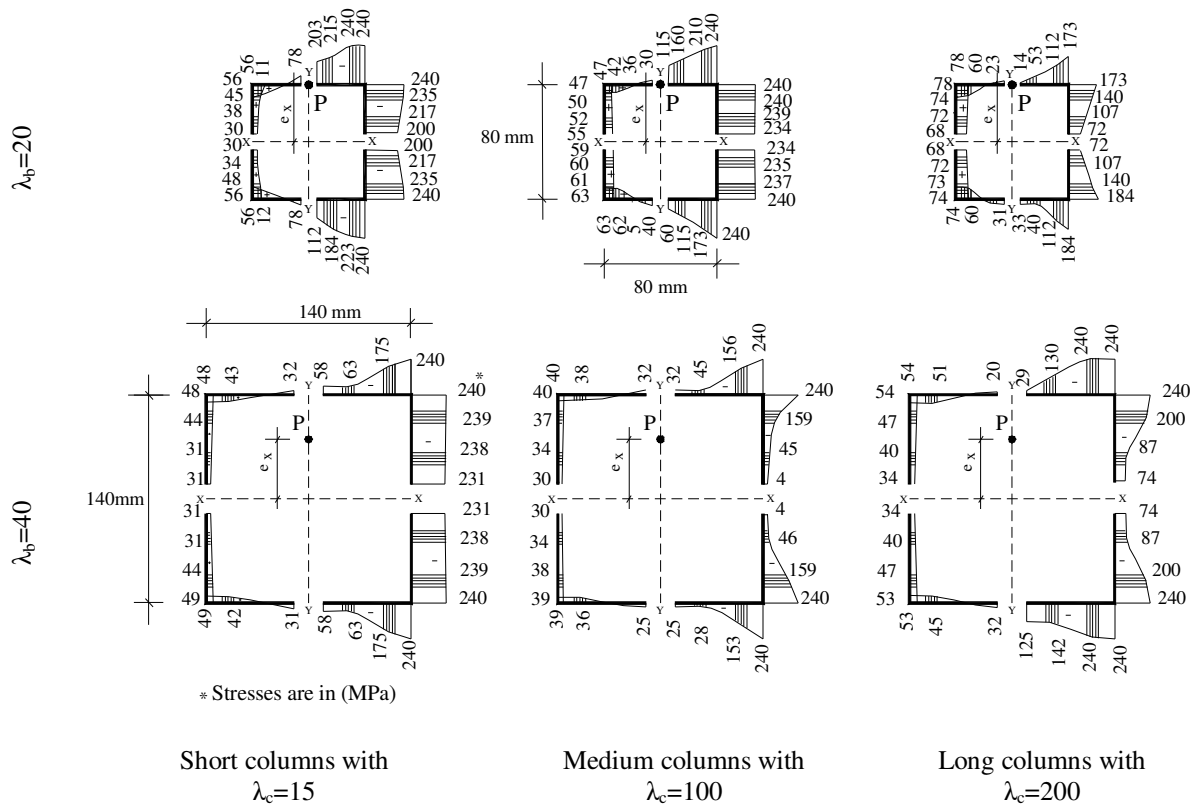
Figure 12: Stress Distribution at Failure Load across the critical section of battened columns subjected to uni-axial load

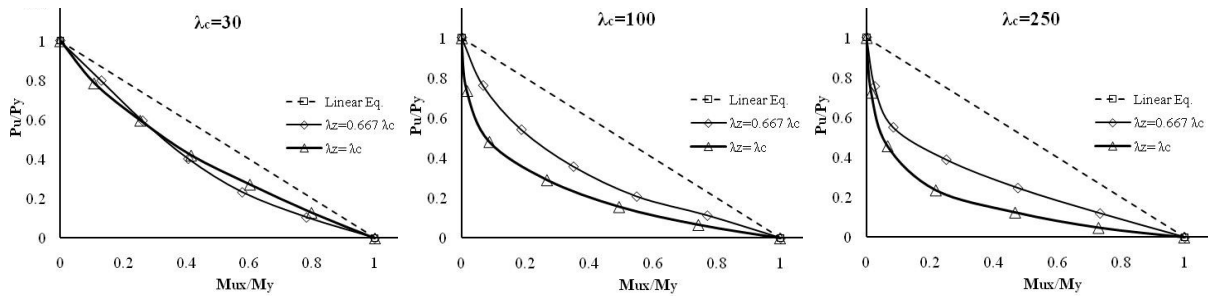## 4.2 Ultimate Axial and Flexural Strengths Interaction Curves

Figure 13: Interaction diagram of uni-axially loaded slender battened beam columns having, λ_b=20 and λ_c=30, 100 &250.

For uni-axially loaded members with different overall slenderness ratios λ_c=30, 100 and 250; the interaction curves between, P_u/P_y and M_u/M_y are shown in Fig.13. The relation is presented for width-thickness ratios λ_b=20, λ_z=0.667λ_c and λc= λ_z. Generally, the relation is convex downward, indicating that the strength decreased when the member is subjected to combined axial force and moments. This reduction in strength is obvious for large values of overall

member slenderness ratios, λ_c=100 & 250. Moreover, the effect of the slenderness ratios of angles between batten plates λ_z is clear for long columns, but for short columns the strength are not much affected by this factor.

4.3 Comparison between Standard Design Specifications and Finite Element Analysis Results
The finite element ultimate strength is compared with the design rules of EC3 (2001) and AISI (2007). As shown in Fig. 14, the relation between P/P_{uo} and M/M_{uo} for uni-axially loaded columns is plotted for different overall slenderness ratios, λ_c, and different width-thickness ratios, λ_b. P_{uo} is the ultimate axial load when there is no end bending moment and M_{uo} is the ultimate bending moment when there is no axial force.
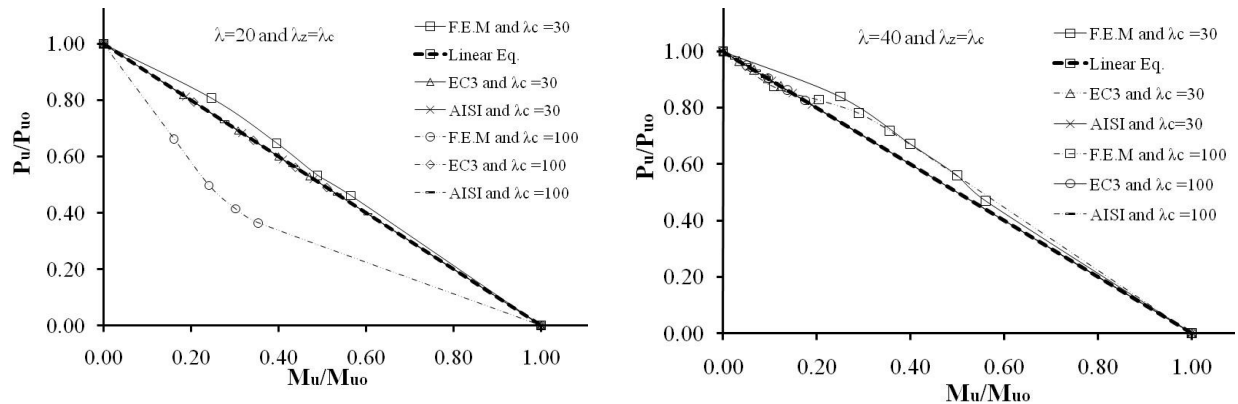

Figure 14: Interaction diagram of uni-axially loaded battened columns subjected to axial as well as bending moment about X-axis with, λ_b=20 & 40 and λ_z= λ_c =30 & 100.

The linear interaction equation, $P/P_u+M/M_u$=1.0, is drawn in the same figure. For uni-axially loaded members having λ_b=20, 40 and λ_z= λ_c =30; the relation is convex upward and higher than the linear interaction equation. For members λ_b= 40 and λ_z= λ_c =100, the relation is approximately linear. On the other hand, for members having λ_b=20 and λ_z=λ_c =100; the relation is concave downward and less than the linear interaction equation. It is clear that the EC3 and AISI design rules provide good agreement with the finite element analysis results.

5. Conclusions

The ultimate capacity of battened beam-columns composed of four equal slender angles is determined using a non-linear finite element model. Moreover, the local and overall geometric imperfections are measured, in addition to the residual stress patterns of two cold formed angles. Data showed that the average local imperfections range from b/50 to b/20 with highest frequency value of b/15. Moreover, the overall geometric imperfections range from L/1600 to L/284 and also the highest frequency value is L/500. The average residual stress pattern measured is characterized by high tensile stresses concentrated near the corner of the angle with average value ranging from 0.186 F_y to 0.7F_y, and compressive stresses spread near the middle of the angle legs with average value ranging from 0.143F_y to 0.297F_y. Also, results declare that, the ultimate strength decreases by increasing the overall imperfection value. Moreover, the reduction in strength increases by increasing the section width-to-thickness ratio, λ_b, and also the member slenderness parameters. However, for columns subjected to eccentric loads, the effect of the

overall geometric imperfections becomes less important. In-addition the residual stresses reduce the ultimate strength by about 15%.

The finite element analysis of the uni-axially loaded battened beam columns declare that, The local buckling of angle legs on compression side of column deformed shape is very clear for short and medium columns having angle local slenderness ratios, λ_z, equal to the overall column slenderness ratios, λ_c. However; for long columns; failure is governed by the overall buckling failure mode. Moreover, the smaller the axial force that acts at big eccentricity on column cross section, the smaller is the capacity of section. On the other hand, the maximum capacity of column cross section occurs when the column is axially loaded. Furthermore, the linear axial-bending interaction equation is safe and suits the ultimate capacity of members having small, intermediate overall slenderness ratios λ_c and large outstanding leg width-thickness ratios λ_b. However, it is conservative for members having small values of λ_b and intermediate ratios of M_u/M_{uo}. Finally, the Eurocode-3 and AISI-2007 design codes provide good agreement with the finite element analysis results for columns cross-sections with large outstanding leg width-thickness ratios λ_b.

6. Notations

a = Distance between batten plates (interconnectors).
B = Outer dimension of battened column cross section.
E = Young's modulus of elasticity.
f_y = Yield stress.
f_u = Ultimate tensile strength.
I = Minimum Radius of gyration of battened column section.
i_z = Radius of gyration of a single angle.
L = Overall column length.
L_z = Length of angle between centers of batten plates.
P_n = Nominal load.
P_y = Yield load.
λ_c = Battened column overall slenderness ratio.
λ_b = Angle leg width-to-thickness ratio.
λ_z = Slenderness ratio of angle between batten plates.
λ_m = Modified slenderness ratio for battened columns.
Δ = Amplitude of out of plane initial imperfection.
M_{x-x} = Applied bending moment about x-axis.
M_{ux} = Ultimate bending moment about x-axis.
M_y = Yield bending moment.
M_n = Nominal bending moment.
M_u = Ultimate bending moment.
P_u = Ultimate axial load.
P_{uo} = Ultimate axial load when there is no end bending moments.
M_{uo} = Ultimate bending moment when there is no axial load.
b/δ = Local geometric imperfections.
L/Δ = Overall geometric imperfections.

References

AISI (2007), Cold-Formed Steel Design Manual, *American Iron and Steel Institute*, AISI.

B.W.Schafer, T.Pekoz. (1998) "Computational Modeling of Cold-Formed Steel: Characterizing Geometric Imperfections and Residual stresses" *Journal of Constructional Steel Research,* (47), 193–210.

Ballio G,, Mazzolani F.M. (1983) "Theory and design of steel structures," *Chapman and Hall.*

Dan Popovic, Gregory J. Hancock, and Kim J.R. Rasmussen (1999) "Axial Compression Tests of Cold-Formed Angles" *Journal of Structural Engineering*, 125(5).

Desalvo, G.J., and Gorman, R.W. (1989) "ANSYS, Version 10", *Swanson Analysis Systems*, Houston, PA.

El Aghoury M.A, Salem A.H, Hanna M.T and Amoush E.A. (2010) "Experimental investigation for the behaviour of battened beam- columns composed of four equal slender angles" *Thin-Walled Structures*, 48(9) 669-683.

Eurocode-3 (2001), "Design of steel structures", EC3, DD ENV 1993-1-3.

Hasham S.A, Rasmussen J.R.K. (2002). "Interaction curves for locally buckled I-section beam-columns" *Journal of Constructional Steel Research,* (58) 213-241.

 Murray C. Temple and Ghada Elmahdy (1993) "An examination of the requirements for the design of built-up compression members in the North American and European standards", *Can. J. Civ. Eng*, 20(6) 895–909.

Salem A.H, El Aghoury M.A, El Dib F.F, and Hanna M.T. (2004) "Ultimate capacity of I-slender section columns", *Journal of constructional steel research*, (60), 1193-1211.

Sridharan S., and Ali M. A., (1988) "Behavior and Design of Thin-Walled Columns," *J. Struct. Engrg.*, ASCE, 114(1), 103 - 120.

Trahair N.S. (2007). "Behaviour of Single Angle Steel Beams" *Centre for Advanced Structural Engineering*, Research Report No R884.

Weng C. C., and Teoman Pekoz, (1990) "Residual Stresses in Cold-Formed Steel Members, "*J. Struct. Engrg.*, ASCE, 116(6), 1611 - 1625.